Accepted Article – In E.W. Lam and T.D.C., Little, "Angle Diversity to Increase Coverage and Position Accuracy in 3D Visible Light Positioning," *Proc. 2019 IEEE Intl. Conf. on Communications (ICC)*, Shanghai, China, May 20-24, 2019, https://doi.org/10.1109/ICC.2019.8761558.

Angle Diversity to Increase Coverage and Position Accuracy in 3D Visible Light Positioning

E.W. Lam and T.D.C. Little
Department of Electrical and Computer Engineering
Boston University, 8 Saint Mary's St., Boston, MA 02215 USA
(617) 353-9877
tdcl@bu.edu

Abstract: The most common approach to light-based indoor positioning relies on multilateration of received signals to the mobile device. Any deficiencies in the fidelity of these light signals can significantly distort position estimates.

In this paper, we propose a method to dynamically control the light distribution from the overhead luminaires to mitigate fading effects that would otherwise occur under static lighting. By manipulating the direction of the luminaire, effectively the dispersion pattern, we introduce signal diversity in the form of multiple pointing angles and light distributions. In addition to providing angle diversity, steering and then tracking sustains the maximal line-of-sight path between a source and receiver, which reduces angle-dependent attenuation and optimizes the signal-to-noise ratio for any coordinate without needing to change the physical properties of the source or receiver.

This gain in signal strength combats the limited field-of-view of luminaires and photodiodes to provide better overall coverage, which translates directly to increase positioning accuracy, particularly in a 3D space. In the results, we show field-of-view gains of 43% and improvements in MSE of 20cm.

Keywords: Visible Light Positioning, Light-based Positioning, Optical Wireless Communications, Steering, Location-based Services.

 This work is supported in part by the Engineering Research Centers Program of the National Science Foundation under NSF Cooperative Agreement No. EEC-0812056. Any opinions, findings, and conclusions or recommendations expressed in this material are those of the author(s) and do not necessarily reflect the views of the National Science Foundation.

1 Introduction

Indoor geolocation remains an open challenge due to the limitations of available solutions in terms of cost, complexity, robustness, and accuracy. The ideal approach would be easy to deploy, use an existing infrastructure, and would have robust, repeatable performance across a large fraction of the active indoor space. High accuracy can also be important but that depends on the target use case. Included in 'easy to deploy' is self-configuration and self-calibration. The system should be adaptive to changes in the environment. Light-based positioning schemes are favored over RF solutions for their accuracy, line-of-sight (LOS) coverage, and cost [1].

Visible Light Positioning (VLP) approaches in particular also have the benefit of potentially using an existing lighting infrastructure including power, fixture, and the ability to sequester light signals within a space. Future lighting will also incorporate Visible Light Communications (VLC) ensuring active communication from the lights to the devices [2], which is useful in real-time system calibration. In this paper we consider techniques that rely on detecting and decoding incident signals. For example, a mobile phone with a camera or photodetector can receive and interpret coded light from above. In this case the signal quality including strength (received signal strength – RSS) or signal-to-noise (SNR) is important in determining position accuracy and establishing the maximum operating field-of-view (FOV). That is, once a signal becomes noise dominant, that signal is no longer useful.

This operating FOV is typically limited by the distance between the transmitter (luminaire) and receiver (photodetector), the semiangle at half power of the transmitter, and the concentrator semiangle of the receiver. Low-noise hardware can also be used to increase FOV, but with limits. In 2D positioning, the positioning plane is cleverly chosen to maximize the area of the plane while maintaining that each position in the plane is within the FOV of at least three luminaires. The three-luminarie limitation is a design requirement in the most pervasive VLP techniques, e.g., trilateration [3], triangulation [4], fingerprinting [5, 6], and imaging [7, 8]. In fact, in a recent comprehensive survey of the state-of-the-art VLP techniques, only four of the thirty-five surveyed techniques use a single luminaire to position [9]. However, in 3D the maximum lateral FOV – a 'cone' shape – shrinks for points closer to the ceiling. This makes satisfying the three-luminaires requirement difficult and greatly hinders the performance of multi-luminaire positioning in 3D [10]. Leveraging the existing lighting systems also introduces FOV limitations, as lights are typically deployed to meet lighting needs and standards, and are not usually intentionally positioned for VLP. Operating in the regime where multipath is negligible is also preferred [11].

Recent advancements in lighting include innovations to dynamically steer the direction and emission pattern of light. We propose to use this innovation to steer light to any angle within a fixed range and resolution; and thus to effectively provide angle diversity at the transmitter. The VLC community has started to explore the benefits of steerable lighting [12, 13]. Consequently, we also can take advantage of this angle diversity. Our approach is to use an initial position estimate derived from fixed angle estimates (e.g., from beaconing [14]) and then use the initial position estimate to iteratively steer the lights for

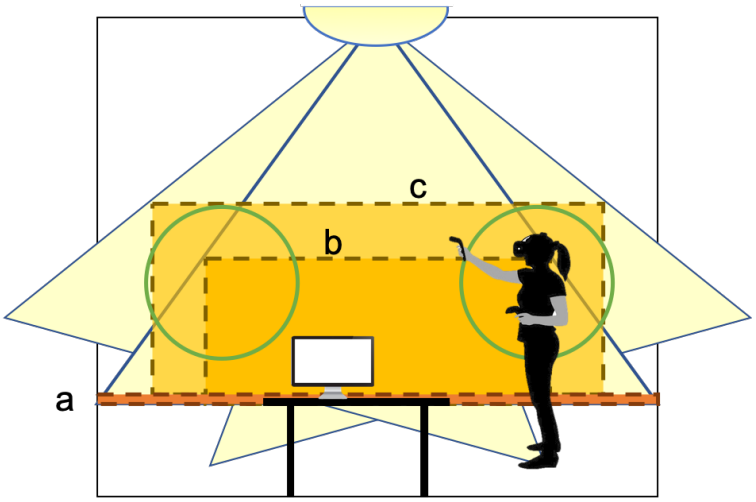

Figure 1: (a) 2D positioning constraint without steering, (b) 3D positioning constraint without steering, and (c) 3D positioning constraint with steering.

better SNR and subsequently improved position estimate. Fig. 1 shows a simplified example of this benefit, highlighting three scenarios: (a) the 2D positioning plane limited by the FOV of the unsteered light, (b) the 3D positioning volume limited by the FOV of the unsteered light, and (c) the increased 3D positioning volume with the same FOV but with steering.

We envision the use case of dynamic steerable luminaires for positioning in situations serviced by dynamic steerable VLC [12, 13]. In such use case, the positioning capability is a mostly cost-free feature. Applications that would benefit from data connectivity and positioning include VR/AR headsets, work spaces where activity and devices are where the light steers to, warehouse robots, and drone fleets to name a few. There may even be niche cases where visible spotlighting is desired – IoT fitness wearables on ballerinas. It is also possible to steer the luminaires quickly without detriments to illumination to service multiple devices, spreading the cost of the devices across multiple users.

This paper explores the intricacies of steering luminaires, Lambertian sources, for better positioning accuracy. We start by investigating the channel model and angle dependency of Lambertian light sources. We show the current FOV limitations and then how FOV can be increased with steering and the subsequent increase in RSS. Next, we propose a way this FOV gain can be exploited for position accuracy gains using an iterative approach. Finally, we show experimental results using a small-scale prototype to validate the quality of our signal model and simulate two VLP techniques: a multi-luminaire benchmark, multilateration [3], and a single luminaire benchmark, Ray-Surface Positioning (RSP) [15].

The remainder of the paper is organized as follows: Section 2 describes the channel model and its dependency on angle and the resulting FOV and SNR; Section 3 highlights how this increase in FOV and SNR can be translated into gains in positioning accuracy; Section 4 gives results experimentally and simulated; Finally, Section 5 concludes the paper.

2 Lighting Coverage

In this section we describe the illumination model of Lambertian sources and the resulting signal received at a photodetector. We focus on the angle dependency as this is the parameter that steering affects.

Different lighting scenarios (sources and receivers) as well as where and how far away these devices are from each other will result in different lighting coverage and subsequent receiver SNRs. Luminaire FOV is determined by a cutoff SNR where noise becomes dominant. Given dynamically steered lights, for the best SNR possible for any given luminaire and photodiode, SNR is improved and thus FOV is edged outward and position accuracy increases without the need to increase power at the source or decrease noise at the receiver. This increase in signal power occurs as a result of reducing angle dependent attenuation losses. The following section describes where this angle dependency arises from and how it impacts SNR.

2.1 LOS Channel Model

The dominant, LOS, received signal at a receiver is a function of the channel model at a position plus noise, defined:

$$P_r = P_t H_{LOS}^{DC} + N, \tag{1}$$

where P_t is the transmitter power for a luminaire, H_{LOS}^{DC} is the LOS Lambertian channel model, and N is noise, typically AWGN from shot and thermal noise. For $0 \leq \psi \leq \Psi_c$, where Ψ_c is the FOV semiangle of the concentrator, the LOS channel model is defined as [16]:

$$H_{LOS}^{DC} = \frac{(m+1)}{2\pi} cos^m(\phi) \frac{A}{d^2} R_{eff}(\psi) * cos(\psi), \tag{2}$$

where d is the Euclidean distance between the transmitter and receiver, ϕ and ψ, shown in Fig. 2, are the angles between the transmitter and receiver measured normal to each respectively, R_{eff} is the effective responsivity of the photodiode, which we assume is constant, and m is Lambertian order calculated with respect to the the transmitter semiangle at half power, $\Phi_{1/2}$, [16]:

$$m = -\left[\frac{ln(2)}{ln(cos(\Phi_{1/2})}\right]. \tag{3}$$

Without changing the transmitted power and noise in a system, you can decrease attenuation losses in the channel by changing the angle of the transmitting luminaire (i.e., steering the luminaire). This impacts the first cosine function associated with the transmitter angle, ϕ, and Lambertian order, m, known as the Lambertian Radiant Intensity, L [16]:

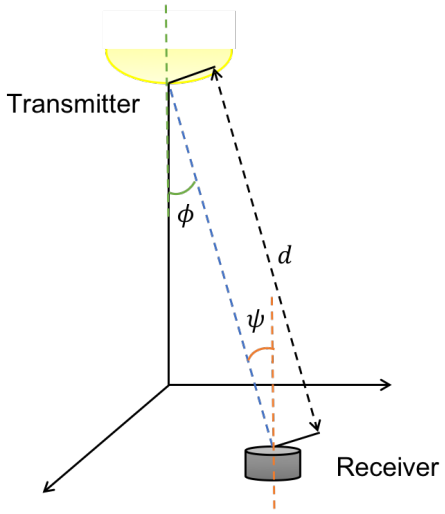

Figure 2: Typically, if the receiving plane and transmitting plane are parallel, $\phi = \psi$. However, with steering, ϕ changes while ψ remains constant.

$$L(\phi) = \frac{(m+1)}{2\pi} cos^m(\phi). \tag{4}$$

Given a typical value for the FOV of the receiver concentrator, $\Psi_c = 60°$, the difference in transmitted power can be a difference of half, i.e., $cos(0) = 1$ and $cos(60) = 0.5$ for perfect steering from $\phi = 60°$ to $\phi = 0°$ and Lambertian order, $m = 1$.

Fig. 3 plots the Lambertian Radiant Intensity L and shows the angle dependency for different transmitter Lambertian orders, i.e., if a source has a Lambertian, $m = 2$, and a different source has a Lambertian order, $m = 1$, a receiver at angle, $\phi = 30°$, will receive less power from the source with Lambertian order, $m = 2$, given the rest of the parameters are the same. The note of emphasis here is that the greater the angle between source and sink, but still within the FOV, the more power is attenuated. The cases with large angles are typically the cases closer to the ceiling and in the corners of the room. Consequently, cases closer to the ceiling and in the corners of the room have poor signal power and poor positioning accuracies due to the wide angle the receiver is from the light. Also note that steering at greater angles results in more diversity; the slope of line is greater for larger angles. This increase in diversity will increase positioning accuracies more significantly when steering large angles, i.e., steering is more impactful for large angle deviations from normal, which occur when positioning closer to the ceiling and in the corners of the room.

2.2 FOV Restrictions on 3D Positioning

One aspect of light-based positioning often neglected is the combined transmitter and receiver FOV limitation. On the receiving end, if the ψ angle between the transmitter and receiver is greater than the FOV of the receiver's concentrator, Ψ_c, then signal is simply not received.

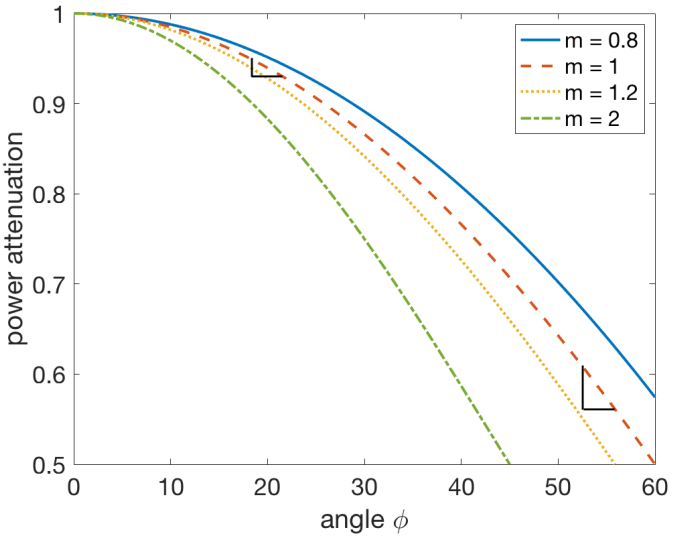

Figure 3: Power attenuation due to angle dependency for different lambertian orders. Power attenuation is not linear and the slope is greater at larger angles. As expected, the slope of attenuation is greater for narrower beams.

In the case where there is no concentrator, the physical limitation angle is 90°. However, on both the transmitter and receiver side, once the angle between the two is past the FOV semiangle of the transmitter and 60° for a concentrator-less receiver, or the FOV semiangle of a receiver with a concentrator, the attenuation factor due to angle is larger than half for each due to the signal attenuation relationship being regulated by cosine functions for both. Together, this is larger than 75% attenuation and increasing exponentially the greater the angle is from those limiting angles. As a result, in 2D positioning, the spacing of lights is typically so that each coordinate within the positioning space is within 60° of a luminaire. This concept was alluded to in the introduction of this paper, in Fig. 1, where the FOV is fixed at $-60°$ to 60° with respect to the transmitter's normal axis but the lateral distance of the FOV shrinks as it moves closer to the light.

In 2D positioning, staying within this 60° constraint is dependent on the vertical height dimension: the further away in the vertical dimension, the larger the lateral spacing. Nevertheless, in 3D positioning scenarios, positioning is sometimes required closer to the ceiling (e.g., an AR/VR headset worn standing up). Bringing the receiver closer to the ceiling increases angle attenuation. In contrast, bringing the receiver closer to the ceiling also reduces distance away from the transmitter. Thus there is a square distance dependency that would in theory offset the decrease in signal due to angle when brought closer to the light. Fig. 4 shows this tradeoff between height and angle at two lateral distances away from the transmitter, $1m$ (solid lines) and $3m$ (dotted lines). In Fig. 4, the percentage of remaining power due to angle and the height of a transmitter is plotted where 100% corresponds to no loss and 0% corresponds to full loss. The blue lines show perfect steering where there is zero attenuation due to angle and losses are due just to height. The green lines show losses due to height and angle. It is shown that moving closer to the ceiling without removing angle-dependent attenuation loss is never better than removing the angle-dependent attenuation.

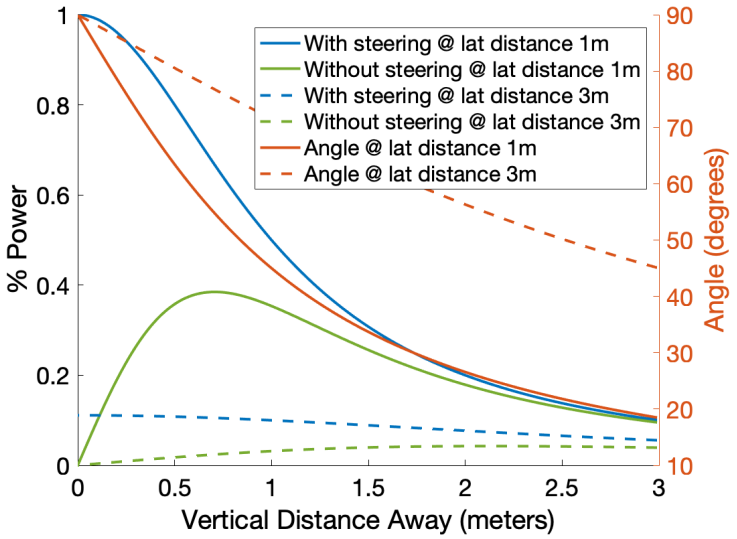

Figure 4: Remaining power for two cases: steered (zero angle attenuation) and unsteered at fixed lateral positions, $1m$ and $3m$, for varying heights, vertical distance away from the luminaire. This shows that reducing angle attenuation has more of an impact than reducing vertical distance away from luminaire.

But there are locations where steering has minimal impact as the distance attenuation is overwhelming large. These cases occur when the receiver is far away in height, e.g., $3m$ away, demonstrating that steering helps position at corners but not corners at floor level. Fig. 4 also shows steering to have a larger impact on lateral distances closer to the transmitter. This is due to the high angle change in slope. The red lines show a larger slope change for $1m$ lateral distance than $3m$ lateral distance.

The full effects of steering and conventional unsteered light on FOV can be seen in Fig. 5. Fig. 5(a) shows the coverage of one luminaire for an unsteered configuration. In this coverage, we carve out a positioning volume (represented in 2D) of acceptable signal strength to overcome a given noise level. In Fig. 5(b) the same luminaire is steered to the device and now the positioning volume has extended in height and lateral dimension for a total increase in area of 55%. The receiver impact still attenuates, but the transmitter attenuation is recovered. Thus, the steered configuration is now suited for the typical configuration of modern lighting, where lights are spaced $2m$ apart from each other. In order for the unsteered configuration to accommodate the same space, the density of the lights would need to increase, which is not always possible. Steering allows for more flexibility in carving out a 3D space with an acceptable luminaire spacing and illumination.

The importance of FOV is that in the case where the target device is not within the FOV of any of the luminaires, the device cannot use LOS signals for positioning. As a result, multi-luminaire positioning schemes (e.g., using trilateration, triangulation, imaging) will fail.

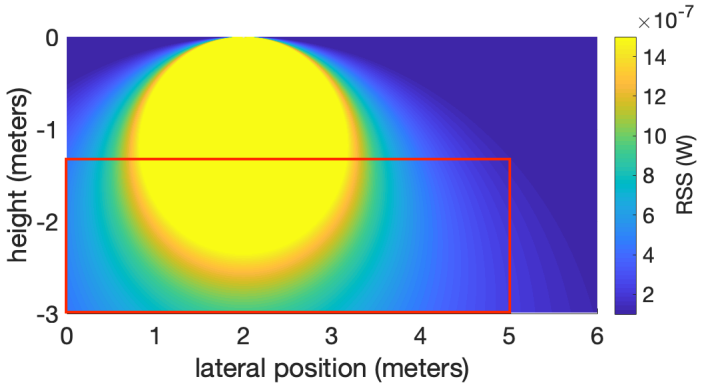

(a)

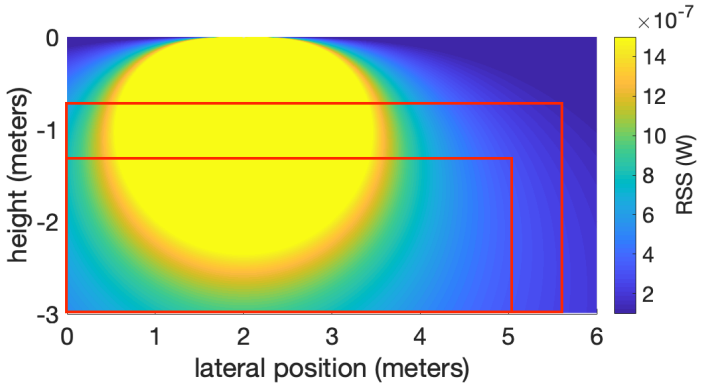

(b)

Figure 5: (a) Unsteered coverage for $m = 1.12$ and (b) steered coverage for $m = 1.12$. Coverage increases by 55% allowing for a wider 3D space.

2.3 SNR Increases with Steering

In addition to the increased FOV, steering the luminaires reduces angle dependent attenuation to zero, which ensures the target device receives the greatest signal possible for a given coordinate. This increase in SNR translates directly to position accuracy gains for RSS-based positioning systems.

Fig. 6 shows two different RSS coverages for a transmitter fixed at a height of $3m$ away from the ceiling and lateral coordinates of $(1.5m, 1.5m)$ with the difference between the two surfaces being whether the lights are steered perfectly to the apex of the cosine function or not. Fig. 6 demonstrates that steering the lights raises the raw signal strength level and thus improves SNR. As expected, due to the cosine dependency, the increase in RSS is greater for the larger angles, which in this case are locations further away from the source. Directly underneath the transmitter where steering is not needed, there is no gain in signal strength.

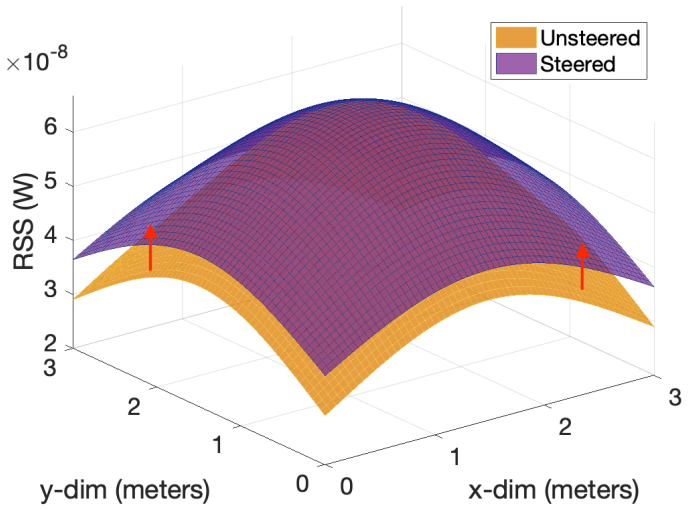

Figure 6: Received signal power for unsteered and steered lighting for a single luminaire and $m = 1.12$. The steered luminaire creates a different RSS value corresponding to the same coordinate in the space.

3 Iterative Steerable Lighting VLP

Based on the analysis in Section 2, we design an approach to make position estimates using angle diversity with steerable luminaires. In order to maximize SNR, the Lamberitan radiant intensity, Eq. 4, is optimized for angle ϕ. Since Eq. 4 is cosine regulated, $\max\{cos^m(\phi)\}$ occurs when $\phi = 0$. Physically, this happens when the transmitter is steered so that its angle normal to the ceiling, Δ, is the same as the angle between the transmitter and receiver when in the home, unsteered, configuration, ϕ_1, i.e. when $\phi_1 = \Delta$.

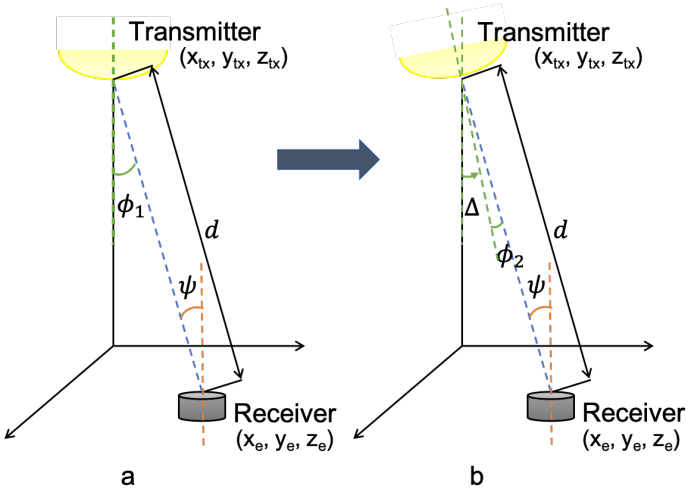

Figure 7: (a) Home geometry, (b) steering geometry. Here, $\phi_2 = \phi_1 - \Delta$, while d, ψ, and ϕ_{laser} remain the same.

In practice, ϕ_1 is not known prior to estimating position. Therefore, Δ can be arbitrary determined or, the more practical approach, calculated based on an estimated position using a simple VLP scheme and the transmitter position:

$$\Delta = tan^{-1}\left(\frac{\sqrt{|x_e - x_{tx}|^2 + |y_e - y_{tx}|^2}}{|z_e - z_{tx}|}\right), \tag{5}$$

where x_e, y_e, z_e are the estimated coordinates of the target receiver and x_{tx}, y_{tx}, z_{tx} are the coordinates for a known transmitter. Since it is not guaranteed that the steered Δ is equal to ϕ_1, we calculate a new angle for the steered configuration: $\phi_2 = \phi_1 - \Delta$. Finally, the channel model is adapted for this steered angle deviation:

$$H_{LOS}^{DC} = \frac{(m+1)}{2\pi} cos^m(\phi_2) \frac{A}{d^2} R_{eff}(\psi) * cos(\psi). \tag{6}$$

This new iteration of the channel model is used in place of the original channel model to predict position using any various positioning schemes. Although the transmitter angle, ϕ, has changed, the other parameters (m, d, A, ψ) have remained constant as the receiver is assumed to have not moved during steering, i.e., $\psi_1 = \psi_2 = \psi$ and $d_1 = d_2 = d$.

Fig. 7 shows the geometry for the unsteered home configuration used with the original channel model and then the steered configuration detailing ϕ_2 used in the steered channel model. Any positioning scheme will benefit from the increased FOV and SNR provided by steered lighting but we will focus on a multi-luminaire example, multilateration [3], and a single luminaire example, RSP [15]. In practice, VLC will provide real-time communication of the current steered angle, Δ, to the receiver.

4 Results

In this section, we first show a small-scale experiment to verify the FOV and SNR increases due to steering. Next, we describe simulation parameters and show simulation results for positioning with steering for two positioning schemes: multilateration and RSP.

4.1 Experimental Signal Verification

To evaluate the feasibility of using steerable lighting, we conduct a small-scale experiment as a proof of concept. Our test apparatus is comprised of a CREE XLAMP MC-E LED chip which consists of four LEDS: red, green, blue, and white with at total output of approximately 200 lumens at 350mA. We built a computer-controlled pan and tilt actuator with inexpensive servos, SG92R, and 3D printed mounts for the MC-E LED. The MC-E has a full-width-half-maximum (FWHM) of 115°, which corresponds to a Lambertian order $m = 1.12$. For the

photodiode, we mount a Thorlabs PDA36A PIN photodiode parallel to the floor and LED, in an apparatus that can be manually adjusted for changes in the photodiode's X and Z positions. The received signal is fed into an Ettus N210 software defined radio connected to a computer for processing. This setup is shown in Fig. 8.

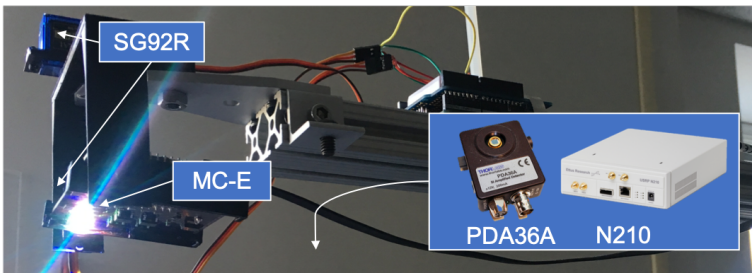

Figure 8: Steerable luminaire setup detailing servos, LED, and photodiode.

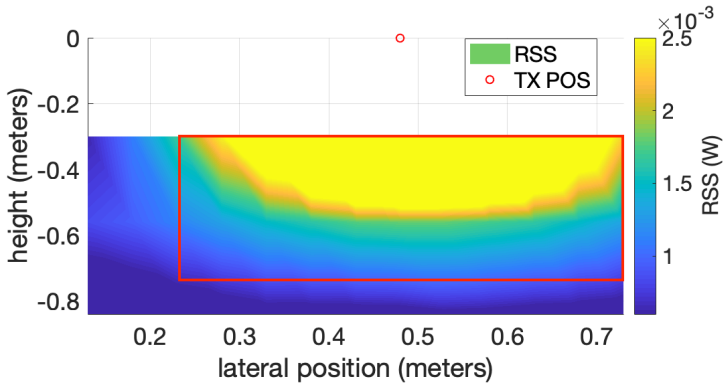

(a)

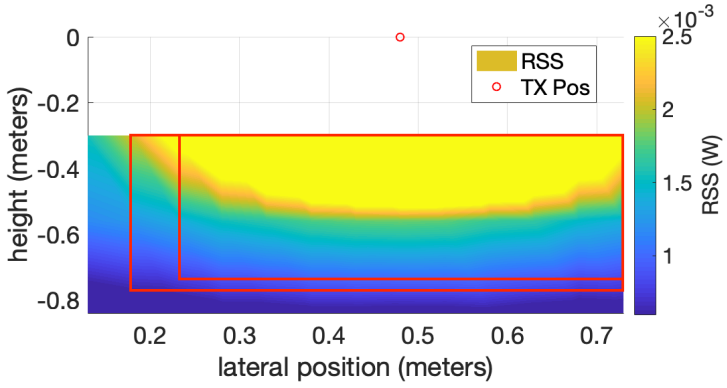

(b)

Figure 9: (a) Unsteered experimental coverage for $m = 1.12$ and (b) steered experimental coverage for $m = 1.12$. Coverage increases by 43%.

Fig. 9 shows collected RSS data of a 2D plane that includes height and one lateral dimension for unsteered and steered experiments. The collected data are at heights: $0.3m, 0.56m$, and $0.84m$, and lateral positions spaced $0.05m$ from $0.13m$ to $0.73m$. Similar to Fig. 5, we isolate a positioning space to meet a threshold of signal strength. And again similar

to Fig. 5, the space extends showing the increased FOV achieved with the introduction of steering. For our test case, coverage is increased by 43%. This increase in RSS is consistent with our predictions that steering will improve the overall coverage even with low-resolution steering. These experimental results give us confidence to explore large-scale simulations for 3D positioning using our proposed method.

4.2 Positioning Simulation Parameters

Here we describe the parameters for simulating our physical model. Recall that we are considering two cases: multilateration and RSP. Multilateration assumes a configuration of four luminaires whereas the RSP method assumes one luminaire. Therefore, to normalize the power, each luminaire in the multilateration configuration is a quarter of the power of the one luminaire in the RSP configuration. Multilateration also requires multiplexing and demultiplexing of the transmitted signals via time-domain or frequency-domain multiplexing. Table 1 shows the parameters used in simulation. For lateral positions, points are evenly spaced from $0m$ to $3m$. Heights are defined for specific results. Steering is assumed perfect.

Table 1: Simulation Parameters

Parameter	**Multilateration Value**	**RSP Value**
TX FWHM	$115°$	$115°$
Area PD	$(3.6mm)^2$	$(3.6mm)^2$
Height	$3m$	$3m$
2D Plane	$3m \times 3m$	$3m \times 3m$
TX Pos	$(1m, 1m)$, $(2m, 1m)$, $(1m, 2m)$, $(2m, 2m)$	$(1.5m, 1.5m)$
Laser Pos	n/a	$(0m, 0m)$
Noise	$-65dB$	-65dB
Power	$15dB/TX$	$20dB$

4.3 Performance at a 2D Horizontal Plane

First, we show predicted performance for a 2D plane $3m$ away from the ceiling of (a) multilateration and (b) RSP. Fig. 10 shows mean square errors (MSE) for multilateration and Fig. 11 shows MSE for RSP. Fig. 12 shows the same MSE but in a cumulative distribution function (CDF) view for both positioning schemes.

For both multilatertion and RSP, there are improvements in positioning error when using the steering method. Since multilatertion requires at least three transmitters, the gains are demonstrated across the entire plane. For RSP, the gains are primarily in the outer reach of the transmitter's FOV and near the laser. The larger errors in the corner (Fig. 11), where the laser is located compared to the rest of the space is a byproduct of the RSP scheme.

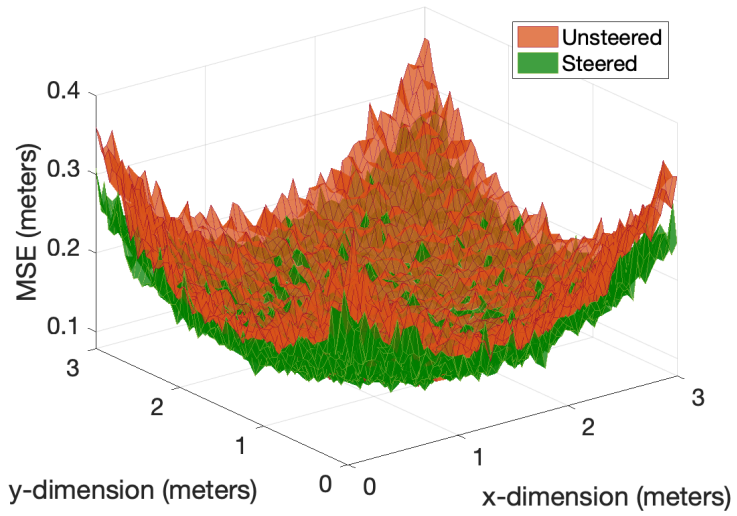

Figure 10: Multilateration: total 3D MSE at $3m$ away from ceiling for steered and unsteered lighting.

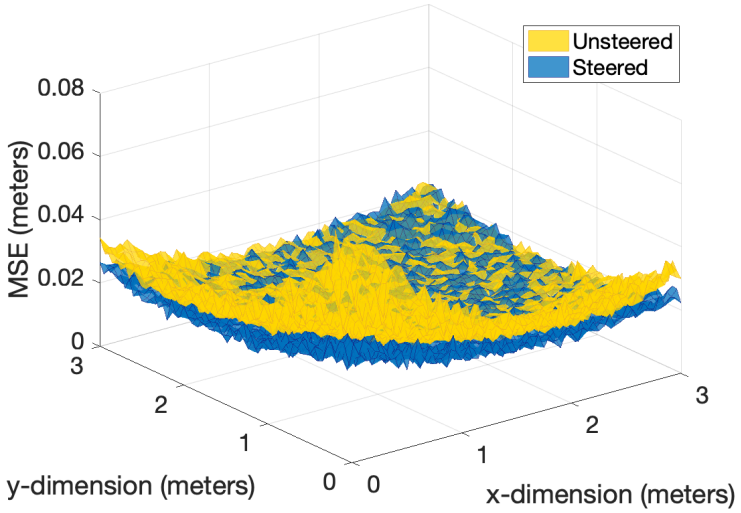

Figure 11: RSP: total 3D MSE at $3m$ away from ceiling for steered and unsteered lighting.

However, positioning is done with a single luminaire, so this anomaly is a compromise. To be clear: the 2D positioning multilateration positioning error here is being compared to a 3D positioning error. Even then, RSP performs better than multilateration due to the one luminaire source being allocated more power than the four individual luminaires. But together, the two configurations provide the same lighting coverage so the comparison is fair.

Fig. 12 shows CDF curves of the MSE at $3m$ away from the ceiling with RSP performing better than multilateration. The purple solid line shows the 95% coverage threshold. The CDF figure shows a better representation of the overall coverage error. Most importantly, in both cases, steering lights improves positioning accuracy using the 95% coverage threshold as a gauge. These results are just for one plane at 3m away. Positioning gains will compound

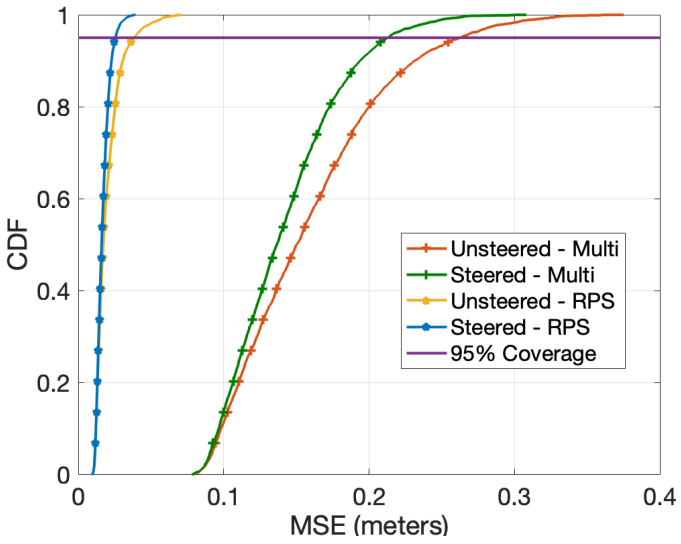

Figure 12: CDF view of errors for RSP and Multilateration for steered and unsteered lighting.

for each plane when considering 3D, especially closer to the lights, which we explore in the next section.

4.4 Performance at Different Heights

Now we abandon the multilateration technique and examine the full room positioning gains with RSP starting with different height planes: $1.5m$, $2m$, $2.5m$, and $3m$ from the ceiling. Assuming the same parameters as the previous section, we run a full room simulation to examine the effects on positioning of steerable lighting throughout a larger space. For this simulation, we keep the location of the laser as the origin and place the luminaire at the center of the room at $1.5m \times 1.5m \times 3m$, which makes sense as this is likely the max space a single luminaire could service.

Fig. 13 shows the full room simulation in two CDF curves: one for unsteered and one for steered. Steering improves positioning accuracy as it increases FOV and SNR. This representation shows what steering can provide in a overall room environment and not just for a particular height. An improvement of $20cm$ in the 3D space is substantial. This is a result of improving FOV as the unsteered configuration does not converge if noise dominant. Another point is that these results are for RSP, which by design is less susceptible to FOV restrictions as it only uses one luminaire. But for schemes such as multilateration, a luminaire would be expected to cover a wider volume, requiring LOS to at least three lights, which is more difficult when the lights are spaced $2m$ apart.

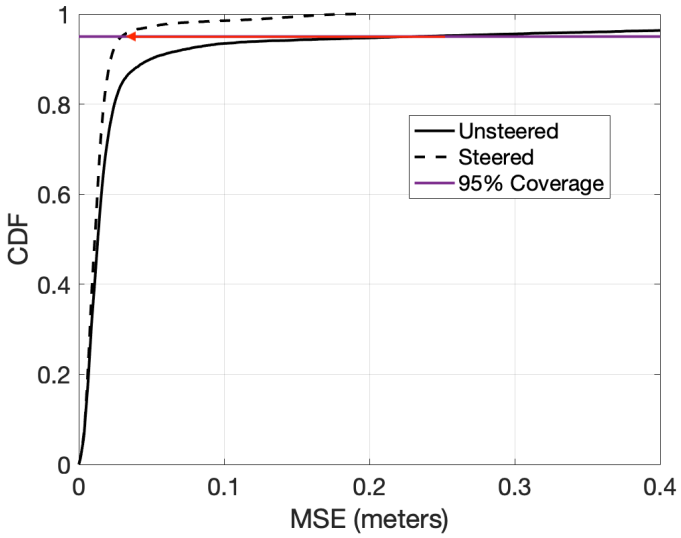

Figure 13: The effects of steering compounded across a 3D space showing a positioning gain of 20cm from unsteered.

5 Conclusion

In conclusion, the adoption of steerable luminaires provides two key benefits for 3D VLP: increasing (1) the illumination coverage of a luminaire and its VLP FOV, and (2) the SNR delivered to the coordinates of a target user device. The FOV increase enables 3D positioning with multiple luminaires while the SNR increase improves the baseline positioning accuracy. We propose that steering the lights will increase the upper bound performance for any positioning algorithm and show in simulation this is true for multilateration and Ray-Surface Positioning. We show that the FOV of the transmitter and receiver are significant parameters in 3D positioning. In our test case, steering increases coverage by 43% and MSE by 20cm. Moving forward, we will continue to investigate and validate the iterative positioning approach both in complexity and convergence and to consider the impact of steering errors in our reported accuracies.

References

[1] J. Armstrong, Y. A. Sekercioglu, and A. Neild, "Visible light positioning: a roadmap for international standardization," *IEEE Communications Magazine*, vol. 51, no. 12, pp. 68–73, December 2013.

[2] H. Elgala, R. Mesleh, and H. Haas, "Indoor optical wireless communication: potential and state-of-the-art," *Communications Magazine, IEEE*, vol. 49, no. 9, pp. 56–62, September 2011.

[3] W. Zhang, M. I. S. Chowdhury, and M. Kavehrad, "Asynchronous indoor positioning system based on visible light communications," *Optical Engineering*, vol. 53, pp. 53 – 53 – 10, 2014.

[4] Y.-S. Kuo, P. Pannuto, K.-J. Hsiao, and P. Dutta, "Luxapose: Indoor positioning with mobile phones and visible light," in *Proceedings of the 20th Annual International Conference on Mobile Computing and Networking*, ser. MobiCom '14. New York, NY, USA: ACM, 2014, pp. 447–458.

[5] J. Vongkulbhisal, B. Chantaramolee, Y. Zhao, and W. S. Mohammed, "A fingerprinting-based indoor localization system using intensity modulation of light emitting diodes," *Microwave and Optical Technology Letters*, vol. 54, no. 5, pp. 1218–1227, 2012.

[6] Z. Vatansever, M. Brandt-Pearce, and C. L. Brown, "Image-sourced fingerprinting for led-based indoor tracking," in *2017 51st Asilomar Conference on Signals, Systems, and Computers*, Oct 2017, pp. 903–907.

[7] B. Lin, X. Tang, Y. Li, M. Zhang, C. Lin, Z. Ghassemlooy, Y. Wei, Y. Wu, and H. Li, "Experimental demonstration of optical camera communications based indoor visible light positioning system," in *2017 16th International Conference on Optical Communications and Networks (ICOCN)*, Aug 2017, pp. 1–3.

[8] R. Zhang, W. D. Zhong, K. Qian, and D. Wu, "Image sensor based visible light positioning system with improved positioning algorithm," *IEEE Access*, vol. 5, pp. 6087–6094, 2017.

[9] Y. Zhuang, L. Hua, L. Qi, J. Yang, P. Cao, Y. Cao, Y. Wu, J. Thompson, and H. Haas, "A survey of positioning systems using visible led lights," *IEEE Communications Surveys Tutorials*, vol. 20, no. 3, pp. 1963–1988, thirdquarter 2018.

[10] E. W. Lam and T. D. C. Little, "Visible light positioning: Moving from 2D planes to 3D spaces (invited)," *Chinese Opticts Letters*, vol. 17, no. 3, p. 030604, Mar 2019. [Online]. Available: http://col.osa.org/abstract.cfm?URI=col-17-3-030604

[11] W. Gu, M. Aminikashani, P. Deng, and M. Kavehrad, "Impact of multipath reflections on the performance of indoor visible light positioning systems," *Journal of Lightwave Technology*, vol. 34, no. 10, pp. 2578–2587, May 2016.

[12] J. Morrison, M. B. Rahaim, Y. Miao, M. Imboden, T. D. C. Little, V. Koomson, and D. J. Bishop, "Directional visible light communication signal enhancement using a varifocal micromirror with four degrees of freedom," in *15th International Conference on Solid State Lighting and LED-Based Illumination Systems*, ser. Proceedings of SPIE, M. Kane, N. Dietz, and I. Ferguson, Eds., vol. 9954, no. ARTN 99540C, San Diego, CA. SPIE-International Society of Optical Engineering, Jan 2016. [Online]. Available: https://doi.org/10.1117/12.2237736

[13] M. B. Rahaim, J. Morrison, and T. D. C. Little, "Beam control for indoor FSO and dynamic dual-use VLC lighting systems," *Journal of Communications*

and Information Networks, vol. 2, no. 4, pp. 11–27, 2017. [Online]. Available: https://doi.org/10.1007/s41650-017-0041-7

[14] P. Lou, H. Zhang, X. Zhang, M. Yao, and Z. Xu, "Fundamental analysis for indoor visible light positioning system," in *2012 1st IEEE International Conference on Communications in China Workshops (ICCC)*, Aug 2012, pp. 59–63.

[15] E. W. Lam and T. D. C. Little, "Resolving height uncertainty in indoor visible light positioning using a steerable laser," in *2018 IEEE International Conference on Communications Workshops (ICC Workshops)*, May 2018, pp. 1–6.

[16] J. Kahn and J. Barry, "Wireless infrared communications," *Proceedings of the IEEE*, vol. 85, no. 2, pp. 265–298, Feb 1997.